
EARLY SCREENING OF SARS-CoV-2 BY INTELLIGENT ANALYSIS OF X-RAY IMAGES

A PREPRINT

D. Gil, K. Díaz-Chito, C. Sánchez, A. Hernández-Sabaté
Computer Vision Center - Dept. of Computer Science
Universitat Autònoma de Barcelona
Cerdanyola del Vallès, 08193
debora@cvc.uab.cat

May 29, 2020

ABSTRACT

Future SARS-CoV-2 virus outbreak COVID-XX might possibly occur during the next years. However the pathology in humans is so recent that many clinical aspects, like early detection of complications, side effects after recovery or early screening, are currently unknown. In spite of the number of cases of COVID-19, its rapid spread putting many sanitary systems in the edge of collapse has hindered proper collection and analysis of the data related to COVID-19 clinical aspects.

We describe an interdisciplinary initiative that integrates clinical research, with image diagnostics and the use of new technologies such as artificial intelligence and radiomics with the aim of clarifying some of SARS-CoV-2 open questions. The whole initiative addresses 3 main points: 1) collection of standardize data including images, clinical data and analytics; 2) COVID-19 screening for its early diagnosis at primary care centers; 3) define radiomic signatures of COVID-19 evolution and associated pathologies for the early treatment of complications.

In particular, in this paper we present a general overview of the project, the experimental design and first results of X-ray COVID-19 detection using a classic approach based on HoG and feature selection. Our experiments include a comparison to some recent methods for COVID-19 screening in X-Ray and an exploratory analysis of the feasibility of X-Ray COVID-19 screening. Results show that classic approaches can outperform deep-learning methods in this experimental setting, indicate the feasibility of early COVID-19 screening and that non-COVID infiltration is the group of patients most similar to COVID-19 in terms of radiological description of X-ray. Therefore, an efficient COVID-19 screening should be complemented with other clinical data to better discriminate these cases.

Keywords COVID-19 · Screening · Xray · Artificial Intelligence

1 Introduction

In the last months, coronavirus SARS-COV-2, which causes COVID-19, has widely spread all over almost all the countries of the world. Due to its high contagiousness, at the present time (19 May 2020¹), the World Health Organization (WHO) confirms a total of 4,731,458 confirmed cases and 316,169 of total deaths all over the world in less than five months, causing a collapse in several health systems. Although the course of the disease is often mild, in a considerable number of cases may lead to a severe pneumonia, among other complications, that can rapidly get worse and require intensive care. Therefore and since there is no effective treatment for COVID-19 yet, early screening of the disease is highly recommended for the identification and treatment high-risk patients, thus, preventing a severe progression of the disease Sun et al. [2020].

¹<https://www.who.int/emergencies/diseases/novel-coronavirus-2019>

There is evidence that Chest CT has a sensitivity for diagnosis of COVID-19 Li et al. [2020], Ai et al. [2020], Wong et al. [2020]. In particular, patients with confirmed COVID-19 pneumonia have typical imaging features that can be helpful in early screening and in evaluation of the severity and extent of disease Zhao et al. [2020]. However, CT is very expensive and difficult to make massively to the population. In contrast, X-ray is a low cost modality based on the same technology as CT which is available at primary care centers. Besides, X-ray allows an affordable rapid triaging that is already being used at hospitals to confirm the disease and monitor patients' recovery since it is a highly available and affordable technique.

The goal of this study is to early diagnose and follow-up patients with COVID-19 from an intelligent analysis of X-ray images. Thus, in this paper we present our general approach for early screening of COVID-19 using X-ray and the first results obtained using a classical approach on a dataset extracted from several public repositories. We describe the sampling strategy for defining a training and testing sets and present the results obtained for Histogram of Oriented Gradients (HoG) descriptor Dalal and Triggs [2015] and a reduction of dimensionality.

Our experiments include the assessment of the most suitable method for dimensionality reduction and HoG parameters, a comparison to state-of-art methods and an exploratory analysis of the capability for COVID-19 early detection. Results show that our approach can outperform deep-learning methods, indicate the feasibility of early COVID-19 screening and identify non-covid infiltration as the group of patients most likely to be radiologically confused as COVID-19. The latter suggests adding clinical variables in order to increase the efficiency of a COVID-19 screening based on X-ray analysis.

The remainder of the paper is structured as follows. Section 2 summarizes the state-of-the-art related with the paper. Section 3 overviews how artificial intelligence can contribute to the fight against the pandemic. Section 4 details the methodology used to early detect COVID-19 in X-Ray images. Section 5 is devoted to explain the experimental setting and show the results assessing our method and, finally, discussion and conclusions are provided in section 6.

2 State of the art

Early detection of COVID-19 from X-rays has risen great interest within the artificial intelligence community. Although results seem encouraging, we consider that there are several issues related to, both, the available data and the experimental design that should be taken into account for fair interpretation of results.

The main radiological feature of COVID-19 (fig. 1 (b), (c)) is the development of pneumonia. Radiologically, pneumonia produces light (white and gray) areas (related to tissue inflammation) inside lungs, which usually show dark due to the low density of their tissue (see fig. 1 (a)). Aside COVID-19, there are several pathologies (like edema or non-COVID pneumonia) having similar radiological description. Unlike other pathologies with similar radiological description, COVID-19 pneumonia has a rapid progression (compare images in fig. 1 (b) and (c)) prone to collapse lungs. At this point, they become completely white in X-ray (see fig. 1 (c)), loose their functionality and the patient requires immediate intensive care assistance. Therefore, a computational system detecting COVID-19 at advanced stages, although probably very accurate, lacks of any clinical value. This implies that data for training and testing methods should be carefully chosen and include, both, COVID-19 early stages and all radiological types similar to COVID-19 associated to other pathologies. Under these considerations, we do a critical review of existing databases and methods.

The most extended public database with COVID+ cases is the one explained in Cohen et al. [2020]. At this moment, it contains 360 frontal view X-rays and CT from 199 different patients with different respiratory pathologies. Images have been extracted from online publications, website, or directly from PDFs, maintaining the quality of the images. The database also contains metadata that includes, for some cases, how many days after hospitalization of the patients images were acquired. Although these offset variable could be considered as an approximation to COVID-19 stage, more clinical data is needed to fully assess COVID-19 stage. The dataset in Dadario contains 20 frontal and lateral X-ray images and CT snapshots of patients diagnosed with COVID-19. All images were extracted from publicly available articles and knowledge bases. The one published in Mooney contains 5863 images of X-ray images with and without pneumonia (no COVID-19). The data base of the Italian society of medical and interventional radiology (SIRM) ² deserves special attention because it contains clinical data, including symptoms, patient data, diagnosis and radiological description from 219 COVID-19 positive images, 1341 normal images and 1345 viral pneumonia images. Although highly valuable from a clinical point of view, a main inconvenience for its use in an artificial intelligence system is that radiographic images have varying resolution and clinical data has not been collected in a systematic manner. Data are the clinical annotations of the physician or radiologist who attended the patient. Thus, it does not always contain the same information and some language parser should be used to identify the different vocabulary used to describe the same pathology.

²<http://www.sirm.org/category/senza-categoria/covid-19/>

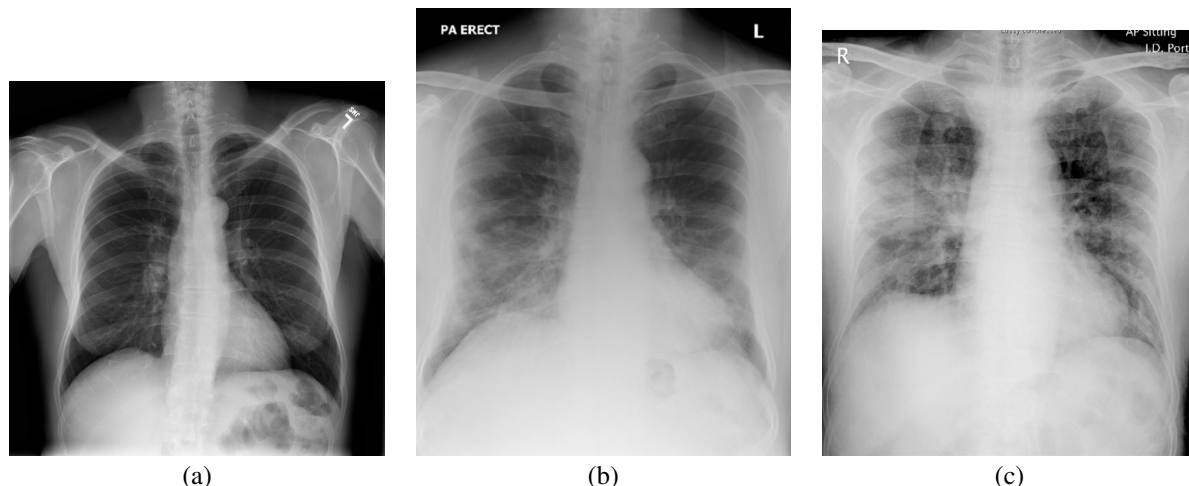


Figure 1: Comparison between Normal and COVID X-ray images: normal case, (a) COVID at early stage, (b), COVID at advanced stage, (c).

A main concern about the above data sources is that they are neither standardized nor record patient’s clinical data such as whether the disease is at an early or advance state. The latter information is mandatory for early diagnosis and follow-up of the disease. As well, some of them (such as Chowdhury et al. [2020]) develop their database from other databases (such as Cohen et al. [2020]) so that merging them to obtain more images does not guarantee non-overlaps between them.

Regarding the methodologies used so far, all of them pose COVID-19 detection as a classification problem. Most use transfer learning to explore the discriminative capability of existing Convolutional Neural Networks Apostolopoulos et al. [2020], Narin et al. [2020], Hemdan et al. [2020], Sethy and Behera [2020], Zhang et al. [2020] already trained with non-clinical databases. Some works replace the deep classifier with a classic one such as SVM Sethy and Behera [2020], Castiglioni et al. [2020] or combine the deep classifier with an anomaly detector Zhang et al. [2020]. The only work presenting an architecture specific to detect COVID-19 is the one described in Wang and Wong [2020]. However, they use again transfer learning and pre-train the network using ImageNet. Concerning the definition and training of the classification problem, most methods Apostolopoulos et al. [2020], Narin et al. [2020], Hemdan et al. [2020], Sethy and Behera [2020], Zhang et al. [2020], Castiglioni et al. [2020], Wang and Wong [2020] define a two class problem (COVID/noCOVID) with the noCOVID class including normal and non-COVID pneumonia for Apostolopoulos et al. [2020], Sethy and Behera [2020], Zhang et al. [2020], Castiglioni et al. [2020], Zhang et al. [2020] and only normal cases for Narin et al. [2020], Hemdan et al. [2020]. The only method training a multiclass problem including normal, nonCOVID bacterial and nonCOVID viral pneumonia and COVID is the own design network described in Wang and Wong [2020]. None of the existing works includes cases with lung infiltration, which radiologically look very similar to a COVID since they are typical in viral pneumonia but can also be originated by other pathologies.

Table 1 details the methodology used in the papers found in the bibliography. In particular, we detail the dataset they use (2nd column), CNN/feature extraction they use, process of transfer learning, if they balance the data or not and the classes considered.

Although results seem promising in most works, there are several issues that should be pointed out. First, the unavailability of a large amount of data is a problem to ensure the reliability of transfer learning, since the images with which networks have been pre-trained can have very different characteristics than we are looking for. Second, the groups considered for the classification problem might not be the most appropriate for COVID-19 early detection. Binary COVID/Normal approaches like Narin et al. [2020], Hemdan et al. [2020] can not assess discrimination between Pneumonia caused by other sources (like bacteria or non-COVID virus), which it is crucial for a reliable screening program. The remaining approaches lack of some radiological descriptions (like infiltration) that are present in viral pneumonia but also in other pathologies and, thus, their capability for discriminating among these pathologies remains unknown. Finally, none of the approaches reports the stage of the COVID-19 cases used. Given that advanced stages are visually easily identified (fig. 1 (c)), these facts can introduce an optimistic bias in the reported accuracy measures.

Another issue introducing a bias in results, concerns the experimental design used to validate and train methods. A main concern is that there is no standardized validation protocol, which hinders fair comparison across methods. The

Article	Dataset	Feature extraction	Transfer learning	Data balance	Classes
Apostolopoulos et al. [2020]	Dataset 1: 224 COVID-19 Cohen et al. [2020] + 700 common bacterial pneumonia + 504 normal Dataset 2: 224 COVID + 714 (400 bacterial +314 viral) pneumonia + 504 normal	VGG19, MobileNet v2, Inception, Xception, InceptionResNet v2	last layer	No	CV/ PNE/ N
Narin et al. [2020]	50 COVID Cohen et al. [2020] + 50 normal Mooney	Inception v3, ResNet50, InceptionResNet v2	1 global avg pooling 2D + 2 FC layers	Not reported	CV/ N
Hemdan et al. [2020]	25 COVID Cohen et al. [2020] + 25 normal Mooney	DenseNet201, VGG19, Inception v3, Xception, MobileNet v2, ResNet v2, InceptionResNet v2	tuning deep learning classifier	Not reported	CV/ N
Sethy and Behera [2020]	collected from GitHub, Kaggle and Open-I repository with unknown number of images	AlexNet, VGG16, VGG19, GoogleNet, ResNet18, ResNet50, ResNet101, Inception v3, InceptionResNet v2, DenseNet201, Xception	1 FC layer + SVM	Not reported	CV/ PNE
Zhang et al. [2020]	100 x-ray images across 70 patients with COVID-19 Cohen et al. [2020] + 1431 x-ray images across 1008 patients with pneumonia no COVID Wang et al. [2017a]	Backbone network: Residual Neural Network + trade off between SVM classifier and anomaly detector	not reported	Augmentation	CV/ PNE
Wang and Wong [2020]	5941 posteroanterior chest radiography images across 2839 patient cases (45 COVID + 1203 normal + 931 bacterial pneumonia + 660 non-COVID viral pneumonia)Cohen et al. [2020]	COVID_Net pre-trained with ImageNet	Not reported	No	CV/ PNE/ N
Castiglioni et al. [2020]	Training: 250 COVID + 250 no COVID, Testing: 74 COVID+ 36 no COVID	ResNet50	last layers, but not reported which ones	Not reported	CV/ PNE

Table 1: Summary of the methodologies used in the state of the art. Different classes are identified as: CV (COVID-19), N (Normal), PNE (non COVID-19 Pneumonia).

experimental design for validation should include a description of the data partition used for training and test, the quality scores for assessment of performance and the statistical analysis carried out.

While some of them assess performance using a k-fold cross-validation Apostolopoulos et al. [2020], Castiglioni et al. [2020], others split data into a single training and test subsets Narin et al. [2020], Zhang et al. [2020] and some directly do not explain the procedure used Hemdan et al. [2020], Sethy and Behera [2020], Wang and Wong [2020]. The only partition that allows statistical analysis of quality scores is a k-fold design.

Concerning quality measures, the most informative scores for clinical assessment of COVID-19 screening are sensitivity (also called recall) and precision (or Positive Predictive Value - PPV). The first one quantifies the percentage of COVID-19 cases that the system detects correctly. The second one quantifies the percentage of cases wrongly detected by the system as COVID-19 from all COVID-19 cases detected. This is relevant if diagnosed cases require further tests in order to confirm the pathology. The remaining scores reported in the literature are not so informative, given that we have a highly unbalanced problem with COVID-19 the minority class. A main concern is that none of the existing studies performs any assessment of the capability for early COVID-19 detection.

Finally, all works (with the exception of Castiglioni et al. [2020]) lack of any statistical analysis. Comparison across the different networks is simply done using average scores, which have not any statistical significance and, thus, it is not guaranteed reproducibility of results in new cases.

Table 2 details the performance evaluation of the methods reviewed in the state of the art. For the performance procedure we also show the data partition in case the authors detail it.

Article	Network	Performance evaluation procedure	Accuracy	Sensitivity (Recall)	Specificity	Precision
Apostolopoulos et al. [2020]	VGG19 Dataset 1	10-fold cross-validation	98.75	92.85	98.75	93.27
	MobileNet v2 Dataset 1		97.40	99.10	97.09	86.38
	MobileNet v2 Dataset 2		96.78	98.66	96.46	NR
Narin et al. [2020]	Inception v3	5-fold cross-validation	97	94	100	100
	ResNet50		98	96	100	100
	InceptionResNet v2		87	84	90	91
Hemdan et al. [2020]	VGG19	Train: validation: test 40%:40%:20%	90	100	80	83
	DenseNet201		90	100	80	83
	ResNet v2		70	40	100	100
	InceptionResNet v2		80	60	100	100
	Xception		80	60	100	100
	MobileNet v2		60	20	100	100
Sethy and Behera [2020]	ResNet50	Train: validation: test 60%:20%:20%, 100 simulations	95.38	97.29	93.47	NR
Zhang et al. [2020]	Backbone	2-fold cross-validation	NR	96	70.65	NR
Wang and Wong [2020]	COVID_Net	NR	83.5	100	NR	80
Castiglioni et al. [2020]	ResNet50	10-fold cross-validation	80	79.72 CI = (72,86)	80.55 CI = =(73,87)	89.39 CI = (82,94)

Table 2: Summary of the experimental design used in the state of the art. NR are not reported results.

3 Project Overview

This project ³ is a collaborative initiative between the Computer Vision Center, and the Research Unit Support of IDIAP Jordi Gol for early diagnosis and follow-up of COVID-19 patients from X-ray imaging analysis. In particular, our initiative has three main objectives:

³<http://iam.cvc.uab.es/portfolio/covair/>

1. *Compile a Standardized Database of COVID-19.* A COVID-19 standardized x-ray database will be collected that includes COVID-19 and non-COVID-19 cases along with the clinical and population data required for computational analysis.
2. *COVID-19 Early Diagnosis.* The goal is to classify x-ray images to discriminate COVID-19 pneumonia from other types of pneumonia. This way, we could provide a screening tool for early and rapid diagnosis at the primary health care level.
3. *COVID-19 Monitoring.* Identify at very early stages normal/non-normal X-ray images with infiltrations and find visual progression patterns that may be characteristic of COVID-19 for predicting possible complications requiring hospitalization.

3.1 Data collection

Patients who have had a chest x-ray in a primary care facility and who have suspected symptoms of COVID-19 will be collected. The following groups of patients will be recruited:

1. Patients with COVID and pneumonia (COVID-19 pneumonia),
2. Patients with COVID-19 and no pneumonia (control group),
3. Patients without COVID-19 and pneumonia (non-COVID pneumonia),
4. Patients suspected of having COVID-19 (unconfirmed) and pneumonia,
5. Patients with respiratory symptoms but no pneumonia (second control group),
6. Patients recovered from COVID pneumonia,
7. Patients recovered from other types of pneumonia (after non-COVID-19 pneumonia).

Data will be collected from prospective and retrospective cases from Catalan primary care centres.

Apart from the imaging data, the following information will also be collected for statistical analysis of population factors: date of each radiograph, date of initial and final diagnosis, gender, age and centre where the images were acquired, and clinical data related to the electronic medical records of each patient. The latter will include the complications that each patient has had in order to develop objective 3 of this project.

3.2 COVID-19 Early Diagnosis

For the diagnostic imaging system, a radiomic artificial intelligence system shall be developed to simultaneously analyze X-ray studies and clinical data. The image analysis system shall be defined to distinguish the different groups and the following technical options shall be considered:

1. Classical classifier RODuda and et al. [1973] based on visual characteristics defined by formulae and filter banks. Although these techniques have a lower accuracy than deep-learning approaches, models can be adjusted with few data. For this system, a radiomic feature space will be defined Lambin and et al [2017] that includes local texture and shape descriptors. Classic radiomic feature spaces such as pyradiomics van Griethuysen and et al [2017], as well as texture descriptors for pattern analysis such as HoG Dalal and Triggs [2015] or LBP Ojala and et al [1996] will be considered. To compensate for the low number of samples (cases), a selection of the most discriminating measurements will be made using linear (PCA, LDA, mRMR) and non-linear (KDCV, KPCA) methods. On this space of low dimensionality characteristics, classical classifiers such as SVM will be applied.
2. Classifier based on deep-learning Schmidhuber [2015]. The number of cases that can be collected in this study discourages a trained model from scratch. Transfer learning strategies will be adopted, but in this case the networks will be trained with public databases of respiratory pathologies (e.g. ChestXray-NIHCC) including some COVID-19 cases (e.g. covid-chest-xray) to then test the features of the deeper layers in the data collected in this study. For the network architecture, we will consider both an auto-encoder trained with non COVID-19 cases to detect COVID-19 cases as anomalies, and a classification network on the different pathologies including covid-chest-xray COVID cases.

3.3 COVID-19 Monitoring

For the system of prediction and prevention of COVID complications, a radiomic signature Lambin and et al [2017] will be defined that considers sequentially all the plates of the same patient. As for the diagnostic system, two approaches will be considered:

1. Classical radiomic signature Lambin and et al [2017]. The descriptors (both radiomic and texture and shape descriptors, as well as deep descriptors) of the diagnostic system will be considered for all sequentially X-rays. A dimensionality reduction that suppresses correlated variables (mRMR) and a logistic regression model with a penalty (such as LASSO or elastic net) will be applied to define the signature most correlated with risk of complication. Different models will be made for each time sequence of x-ray images to determine the minimum number needed to predict a negative evolution of COVID-19 patients.
2. Signature based on neural networks. Recurrent neural networks Schmidhuber [2015] allow the analysis of data sequences and have proven to be effective in a variety of domains (natural language processing, handwriting recognition or genome sequence analysis). As the number of cases that can be collected in this study discourages a convolutional model trained from scratch on the images themselves, a recurrent network will be trained on the visual descriptors extracted for diagnosis. This will allow the definition of simplified architectures omitting the convolutional part and having as input the one-dimensional vector defined by these descriptors. As in the previous point, networks will be trained with both classical and deep descriptors and the number of recurrent layers will be optimized to determine the minimum number of x-ray images needed to predict a complication.

For both objectives, clinical data will be incorporated to detect factors correlated with COVID-19 and increase the discriminative capacity of image analysis. The techniques developed within the Up4Health project led by CVC⁴ will also be applied to decrease the impact of variability in input data associated with acquisition protocols and increase the reproducibility of the diagnostic system. With the aim of generating efficient and adaptable models, an incremental learning architecture will be developed that is capable of evolving the learning model for future mutations of the COVID-19. This incremental approach will be based on dual learning Díaz-Chito et al. [2019], which allows for real time information processing (e-learning).

3.4 Statistical Analysis

To validate which AI strategy gives the best system of diagnosis and prediction of complications, sensitivity, specificity and precision in the detection of COVID-19 and non-COVID-19 cases will be calculated. For each of these quality indicators, an analysis of variance statistical test will be performed to detect differences between the different strategies. In addition, generalized regression models will be used to identify significant clinical factors that correlate with the diagnosis.

4 An Exploratory Approach to Early Detection of COVID-19

From the point of view of machine learning, COVID-19 detection is a small size unbalanced problem Fukunaga [1990], Cohen et al. [2018], being the target class COVID-19 the minority one. Such condition poses a main challenge for accurate performance of machine learning strategies, including deep learning methods. While this can be mitigated by acquiring larger datasets to balance the ratio, being COVID-19 a recent pathology, this is not possible at the moment.

Data augmentation Krizhevsky et al. [2012] has become a standard procedure to improve the training process. Data augmentation schemes increase the number of training samples by simple transformations (like translation, rotation, ip and scale) of the original dataset images. However, the diversity that can be gained from such modifications of the images is relatively small and introduces correlations in training data. These artifacts are prone to drop the reproducibility of machine learning methods, especially in the case of clinical predictions Li et al. [2016].

An alternative to mitigate the curse of dimensionality, it is to apply a dimensionality reduction and feature extraction method Díaz-Chito et al. [2019]. Given the small size of the COVID-19 class in public data bases, we have adopted the latter in a classical approach using hand-crafted features and a SVM classifier Vapnik [2013] with the aim of exploring the feasibility of early COVID-19 detection in X-ray.

In the next sections we explain how we have defined a balanced data set from public data repositories and the proposed feature space.

⁴<http://iam.cvc.uab.es/>

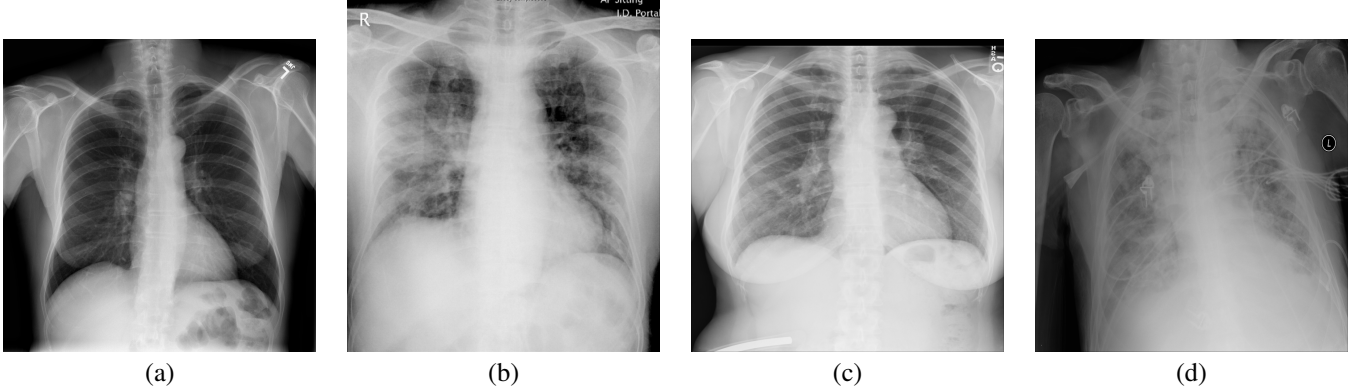


Figure 2: Examples of X-ray images for each class in the data base: normal case, (a) COVID at advanced stage, (b), non-COVID infiltration, (c) and non-COVID pneumonia, (d).

4.1 DataSet Definition from Public Repositories

In this study we have used cases from 2 public repositories: the kaggle database ⁵ and the NIH Chest X-ray Dataset of 14 Common Thorax Disease Categories ⁶ Cohen and Lo [2014], Lo and Cohen [2016].

The repository Cohen et al. [2020] also in kaggle is the most widely used database for COVID-19 detection in X-ray. This database contains front X-ray views from pneumonia caused by several pathogens, including viral and bacterial and an Excel file with metadata of each image. Images have been extracted from online publications, web pages or directly from PDFs, trying to maintain the quality of the images. The data base currently contains 288 X-ray front views from 62 cases (patients) with confirmed COVID-19. For some of the patients, several images taken at different dates are available. The number of days since the start of symptoms or hospitalization for each image is stored in the field offset of the metadata file. This is very important to track progression of the pathology.

The second database Wang et al. [2017b] comprises 112120 frontal-view X-ray images of 30805 unique patients with 14 common thoracic pathologies including Atelectasis, Consolidation, Infiltration, Pneumonia, Edema, Emphysema, Fibrosis, Effusion, Pneumonia, Pleural Thickening, Cardiomegaly, Nodule, Mass and Hernia. The database also includes normal cases labelled as Non-Finding.

To conduct this study, we have created our own dataset containing all cases from kaggle classified in 2 categories (COVID-19 and pneumonia) and a sub-sampling of the NIH Chest X-ray Dataset Infiltration, Pneumonia and Non-Finding. These groups were selected by their potential radiological similarity to COVID-19. Such sub-sampling was randomly selected and of size to balance classes. In total our data set contains 1152 images of COVID-19, Pneumonia, Infiltration and Non-Finding in frontal-view, with 288 images for each class. From now on, these classes will be labelled COVID-19, non-COVID-19 pneumonia, non-COVID-19 infiltration and Normal, respectively. Images have been scaled to 400×400 pixels and normalized in the range $[0, 1]$. Figure 2 shows an example of X-ray image for each class.

4.2 Feature Space Definition

By its capability to describe, both, shape and texture with a low number of parameters we have chosen the HoG descriptor. The technique counts occurrences of gradient orientation in a partition of the image into cells. Counting in each cell is given by the histogram of gradient orientations which are concatenated for all cells to define HoG descriptor.

The only critical parameter of HoG is the size of the cell, since it determines the level of detail (e.g. scale) HoG is able to codify. Also this parameter determines the dimension of the HoG feature space, which equals to $(NRow * NCol) / (CellSize^2) * NBins$, for $NRow$, $NCol$ the rows and columns of the images, $CellSize$ the size of the HoG cell and $NBins$ the number of bins of the histogram of gradients.

Regarding the reduction of dimensionality, we have considered the following methodologies well-suited in case of a number of samples smaller than the dimensionality of the feature space: Principal Component Analysis (PCA), Kernel Principal Component Analysis (KPCA), Linear Discriminant Analysis (LDA) and Discriminant Common Vector (DCV) Cevikalp et al. [2015].

⁵<https://www.kaggle.com/bachrr/covid-chest-xray>

⁶<http://academictorrents.com/details/557481faacd824c83fbf57dcf7b6da9383b3235a>

5 Experiments

In this exploratory study, 4 experiments have been conducted to assess the feasibility of COVID-19 screening using X-ray:

1. *Determine the optimal method for reduction of dimensionality.* For this experiment HoG was applied with $CellSize = 4$. In order to ensure maximum inter class separability, DCV was applied with a fraction of variance to form the pseudo-null space equal to 0.8.

The quality of the reduction of dimensionality was visually assessed by plotting the classes in the space defined by the 3 principal components of each method. Reduction methods were trained using 60% of the data. Visual assessment of the distribution of the remaining test set in the reduced space was enough to discard methods and select the best posed method for the remaining experiments.

2. *Set the optimal scale for HoG descriptor.* In order to set the most appropriate cell size, we have computed HoG with $CellSize \in [4, 8, 16, 32]$. The HoG space was reduced using the method selected in the first experiment. In order to select the optimal HoG scale, we have computed precision (or PPV) and recall (also known as sensitivity). These scores are commonly used in medical imaging applications since they can measure the accuracy in pathology detection in unbalanced settings. If we note TP the number of true positives, FP , the number of false positives, TN the number of true positives and FN the number of false negatives, then precision and recall are given by:

$$Precision = \frac{TP}{FP + TP} \quad Recall = \frac{TP}{TP + FN} \quad (1)$$

Data was managed and analyzed with the software R, version 3.2.5. A different generalized mixed linear model of the effect of each cell size was constructed for each quality. Models included the fold as random effect. We calculated the 95% CI of all scores and p-values. A p-value < 0.05 was considered statistically significant.

3. *Comparison to SoA.* We have compared our method to the recent approaches based on deep learning summarized in Table 1 with the scores reported in Table 2. For the sake of a comparison as fair as possible, we trained 3 different reductions of dimensionality of our HoG with the cell size selected in the second experiment with the classes used for each method in Table 2: 1) COVID-19/Normal for Narin et al. [2020], Hemdan et al. [2020]; 2) COVID-19/non-COVID-19 Pneumonia for Castiglioni et al. [2020], Zhang et al. [2020] and 3) COVID-19/non-COVID-19 Pneumonia/Normal for Apostolopoulos et al. [2020], Wang and Wong [2020]. For each class configuration, we computed average scores for a 10-fold partition.
4. *Capability for COVID-19 early detection.* The capability for early detection was tested by statistical analysis of variance (anova) of COVID-19 detection with data grouped according to the offset into 3 COVID-19 stages: early COVID-19 (offset ≤ 3), mid COVID-19 (offset between 3 and 10) and late COVID-19 (offset > 10). The number of samples for each group was, respectively, 18, 44 and 16. As before, a p-value < 0.05 was considered statistically significant.

In order to compute COVID-19 detections in the whole data set, we aggregated the evaluation of all k-fold models on their COVID-19 test sets. The boolean variable given by a correct detection was the input for the analysis of variance.

The code for all the experiments conducted in this paper is available at <https://github.com/IAM-CVC/CovAIR>. This repository contains Matlab code for the definition of the data base described in 4.1, as well as, one script for each of the experiments. Methods require Matlab PRTools 5.0 toolbox.

5.1 Results

Figure 3 shows the point cloud in the space given by the 3 principal components of each method for the training and test sets for one of the folds. Test samples are labelled adding a "TS" to the name of the class. Methods based on analysis of principal components (PCA and KPCA) perform poorly already in discriminating the training samples. This is expected given that they compute axis capturing the larger variability among samples and these axis are not always the ones that best separate classes. These axis are usual part of the null space of the covariance matrix Cevikalp et al. [2015]. From the two discriminant methods (LDA and DCV), DCV is the one achieving largest separability in training samples thanks to a high fraction of variance that controls the separability in the pseudo-null space. Given that DCV class separability is preserved acceptably in the testing samples, we have selected this method as the most suitable for dimensionality reduction.

Average scores and their 95% CIs for precision and recall for each cell size are shown in Table 3. The highest precision is achieved by $CellSize = 16$, with a $CI = [0.7586902, 0.9105691]$. This size achieves also the second highest recall

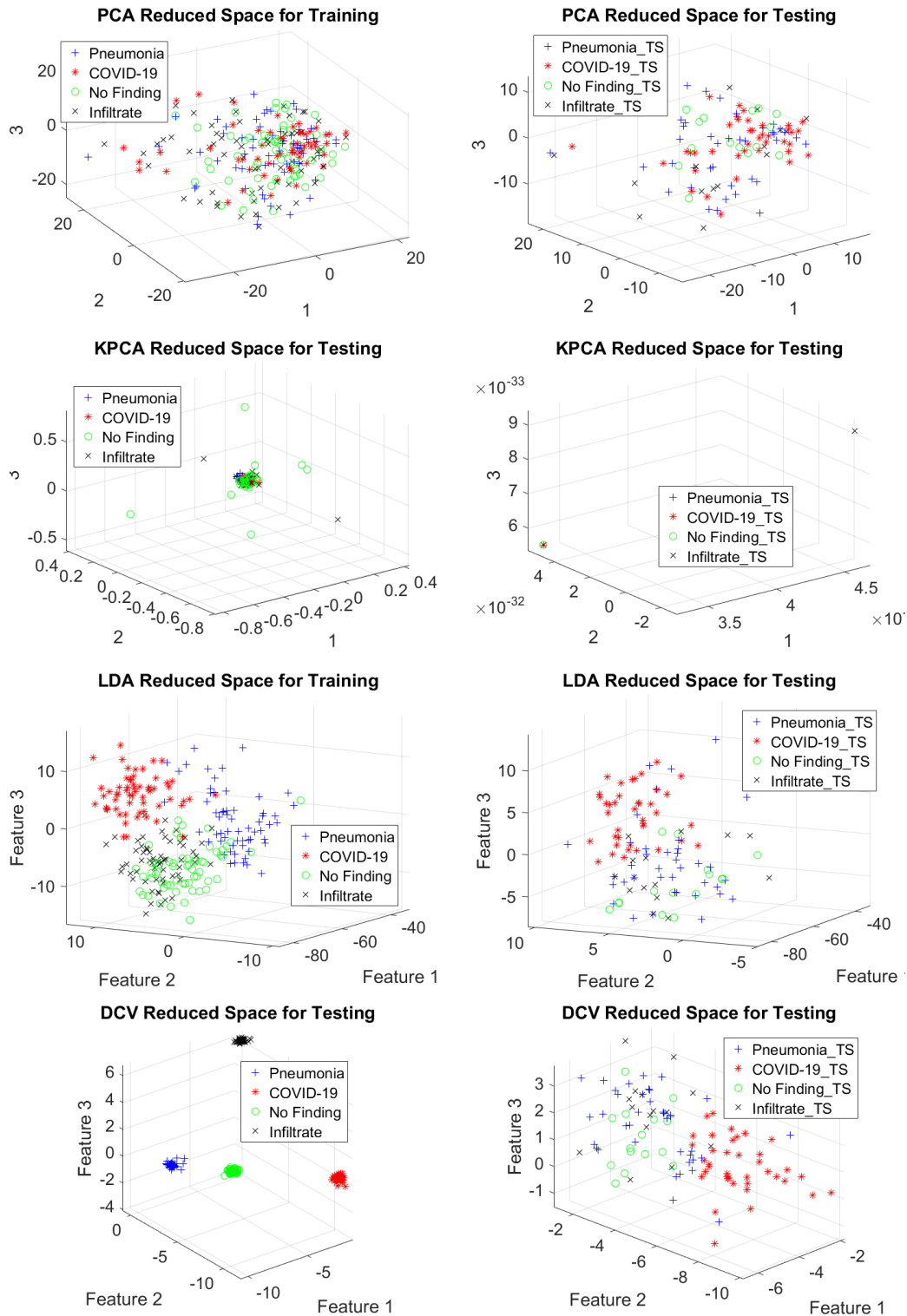


Figure 3: Point distribution in the reduced space given by the 3 principal components of each method. Distribution for training set in left side plots and for testing in right side plots.

with $CI = [0.7999563, 0.9619484]$, which is very close to the highest one achieved by $CellSize = 4$. The p values for the pair wise comparison of cell sizes and confidence intervals for the difference for each score are shown in Table 5.

Significant effects are shown in bold face. The precision achieved by $CellSize = 16$ is significantly better than the one achieved by $CellSize = 4$ and recall is comparable. Although it is not significant, $CellSize = 16$ intervals comparing its precision to the remaining cell sizes have a negative bias and, thus, $CellSize = 16$ tends to have a higher precision. This is also the case for recall intervals. Therefore, we conclude that $CellSize = 16$ is the best suited size for HoG descriptor in images of size 400×400 .

Table 3: Effect of HoG cell size in COVID-19 Detection: average scores

$CellSize$	Precision		Recall	
	Average	95% CI	Average	95% CI
$CellSize = 4$	0.7651227	[0.6891832, 0.8410621]	0.8904762	[0.8094802, 0.9714722]
$CellSize = 8$	0.8031650	[0.7272255, 0.8791045]	0.8476190	[0.7666230, 0.9286151]
$CellSize = 16$	0.8346296	[0.7586902, 0.9105691]	0.8809524	[0.7999563, 0.9619484]
$CellSize = 32$	0.7910462	[0.7151067, 0.8669857]	0.8317460	[0.7507500, 0.9127421]

Table 4: Effect of HoG cell size in COVID-19 Detection: comparison across sizes. Significant effects are shown in bold face

$CellSize$	Precision		Recall	
	p value	95% CI	p value	95% CI
4 – 8	0.2473	[-0.12477274, 0.04868808]	0.1817	[-0.04156023, 0.12727451]
4 – 16	0.0379	[-0.15623738, 0.01722343]	0.7643	[-0.07489356, 0.09394118]
4 – 32	0.4285	[-0.11265393, 0.06080689]	0.0698	[-0.02568721, 0.14314753]
8 – 16	0.3374	[-0.11819506, 0.05526576]	0.2969	[-0.11775070, 0.05108404]
8 – 32	0.7105	[-0.07461160, 0.09884922]	0.6176	[-0.06854435, 0.10029038]
32 – 16	0.1861	[-0.13031386, 0.04314696]	0.1264	[-0.13362372, 0.03521102]

Table 5 reports the quality scores to be compared with the numbers in Table 2. The proposed method achieves average scores above 90% for all configurations of class distribution which are competitive, even better in some cases, to the deep learning approaches reported in Table 2. Comparing to methods considering only the Covid/Normal groups, the proposed method is a bit better than Narin et al. [2020] in terms of recall, with a 4% drop in precision, and much better than Hemdan et al. [2020] in terms of precision. Although the target it is COVID-19 detection and, thus, recall should be high, in a screening problem precision should also be high enough to avoid unnecessary tests to confirm COVID-19. In comparison to methods considering Covid/Pneumonia groups, ours is better than Zhang et al. [2020] in specificity with only 2% in recall and better than Castiglioni et al. [2020] in all scores. Since scores are computed for a two class problem (COVID-19 versus non COVID-19), being our method better in specificity implies that it also has a higher precision. Finally, comparing to methods trained to discriminate Covid/Pneumonia/Normal groups, our method is comparable to Apostolopoulos et al. [2020] in terms of recall with better precision and much better in precision than Wang and Wong [2020] with only 4% drop in recall.

Table 5: Comparison to SoA methods in COVID-19 Detection.

Classes	Accuracy	Sensitivity(Recall)	Specificity	Precision
COVID-19/Normal	96	98	93	96
COVID-19/Pneumonia	93	94	92	95
COVID-19/Pneumonia/Normal	96	98	93	96

Finally, regarding COVID-19 early detection the analysis of variance did not detect any significant differences across the 3 groups with a p-value equal to 0.8284 and average detection rates equal to 89%, 93% and 94% for, respectively, early, mid and late COVID-19 cases.

6 Discussion and Conclusions

In this paper we have presented a method for COVID-19 detection in X-ray based on HoG and reduction of dimensionality. Model parameters include, both, reduction method and HoG cell size and were tuned using statistical analysis of the results obtained for the classification of COVID-19, non-COVID-19 pneumonia, non-COVID-19 infiltration and normal cases. The most suitable configuration was DCV dimensionality reduction and a cell size equal to 16×16 pixels. This model was assessed in 2 aspects: comparison to state-of-art deep learning methods and capability for early detection of COVID-19. The results of our experiments raise some interesting points.

The proposed classic approach is comparable (even better in many cases) to deep learning methods. The accuracy for discriminating among COVID-19, non-COVID-19 pneumonia and normal cases is above 95% with a recall of 98% and a precision of 96%. None of the existing methods included pulmonary infiltration as class, which according to our experiments and clinical evidences might be introducing a positive bias in quality numbers.

Comparing the above results to the accuracy for discriminating between COVID-19 and non-COVID-19 infiltration carried out for model parameters tuning, we have that non-COVID-19 infiltration is the group that most confuses with COVID-19. From a clinical point of view this is expected due to the fact that most non-COVID-19 pneumonia are bacterial and bacterial pneumonia are radiologically very different to a viral one like COVID-19. Viral pneumonia looks like bilateral infiltrations in X-ray. The problem with this is that infiltrations occur in other non-COVID-19 pathologies (acute lung edema, other non-COVID-19 viruses, respiratory distress, etc). Although according to our experiments the number of infiltrations wrongly classified as COVID-19 represent less than 20% of the cases detected as COVID-19 by the system, we consider that these cases should be further filtered using other clinical variables like signs of heart failure (by medical history, physical examination, or analytic).

Regarding early COVID-19 screening using X-ray, our experiments indicate that COVID-19 detection rates is similar at early, mid and late stages of the pathology. However this conclusion should be carefully confirmed using data properly recorded, since the stage of COVID-19 was determined by the number of days past between the start of symptoms or hospitalization and acquisition of each image. Without further radiological description and clinical data this does not guarantee that the first image was acquired at an early stage.

Still, results are very encouraging and, in our opinion, validate the feasibility of early COVID-19 screening using X-ray and, possibly, other clinical variables. The immediate step to fully confirm the actual clinical benefits of this screening is to test our method in retrospective cases collected from Catalan primary care centers.

Acknowledgments

The research leading to these results has received funding from the European Union Horizon 2020 research and innovation programme under the Marie Skłodowska-Curie grant agreement No 712949 (TECNIOspring PLUS) and from the Agency for Business Competitiveness of the Government of Catalonia.

This work was supported by Spanish projects RTI2018-095209-B-C21, fis-g64384969, Generalitat de Catalunya, 2017-SGR-1624 and CERCA-Programme. Debora Gil is supported by Serra Hunter Fellow. The Titan X Pascal used for this research was donated by the NVIDIA Corporation.

"Dedicat a la mama (DGil)"

References

- Qin Sun, Haibo Qiu, Mao Huang, and Yi Yang. Lower mortality of covid-19 by early recognition and intervention: experience from jiangsu province. *Annals of Intensive Care*, 10(1):1–4, 2020.
- Lin Li, Lixin Qin, Zeguo Xu, Youbing Yin, Xin Wang, Bin Kong, Junjie Bai, Yi Lu, Zhenghan Fang, Qi Song, et al. Artificial intelligence distinguishes covid-19 from community acquired pneumonia on chest ct. *Radiology*, page 200905, 2020.
- Tao Ai, Zhenlu Yang, Hongyan Hou, Chenao Zhan, Chong Chen, Wenzhi Lv, Qian Tao, Ziyong Sun, and Liming Xia. Correlation of chest ct and rt-pcr testing in coronavirus disease 2019 (covid-19) in china: a report of 1014 cases. *Radiology*, page 200642, 2020.
- Ho Yuen Frank Wong, Hiu Yin Sonia Lam, Ambrose Ho-Tung Fong, Siu Ting Leung, Thomas Wing-Yan Chin, Christine Shing Yen Lo, Macy Mei-Sze Lui, Jonan Chun Yin Lee, Keith Wan-Hang Chiu, Tom Chung, et al. Frequency and distribution of chest radiographic findings in covid-19 positive patients. *Radiology*, page 201160, 2020.
- Wei Zhao, Zheng Zhong, Xingzhi Xie, Qizhi Yu, and Jun Liu. Relation between chest ct findings and clinical conditions of coronavirus disease (covid-19) pneumonia: a multicenter study. *American Journal of Roentgenology*, pages 1–6, 2020.
- N. Dalal and B. Triggs. Histograms of oriented gradients for human detection. In *CVPR*, 2015.
- Joseph Paul Cohen, Paul Morrison, and Lan Dao. Covid-19 image data collection. *arXiv preprint arXiv:2003.11597*, 2020.
- Andrew M V Dadario. Covid-19 x rays. URL <https://www.kaggle.com/andrewmvd/convid19-X-rays>.

- Paul Mooney. Chest x-ray images (pneumonia). URL <https://www.kaggle.com/paultimothymooney/chest-xray-pneumonia>.
- Muhammad EH Chowdhury, Tawsifur Rahman, Amith Khandakar, Rashid Mazhar, Muhammad Abdul Kadir, Zaid Bin Mahbub, Khandakar R Islam, Muhammad Salman Khan, Atif Iqbal, Nasser Al-Emadi, et al. Can ai help in screening viral and covid-19 pneumonia? *arXiv preprint arXiv:2003.13145*, 2020.
- Ioannis D Apostolopoulos, Tzani A Mpesiana, and Tzani A Mpesiana. Covid-19: automatic detection from x-ray images utilizing transfer learning with convolutional neural networks. *Physical and Engineering Sciences in Medicine*, page 1, 2020.
- Ali Narin, Ceren Kaya, and Ziyne Pamuk. Automatic detection of coronavirus disease (covid-19) using x-ray images and deep convolutional neural networks. *arXiv preprint arXiv:2003.10849*, 2020.
- Ezz El-Din Hemdan, Marwa A Shouman, and Mohamed Esmail Karar. Covidx-net: A framework of deep learning classifiers to diagnose covid-19 in x-ray images. *arXiv preprint arXiv:2003.11055*, 2020.
- Prabira Kumar Sathy and Santi Kumari Behera. Detection of coronavirus disease (covid-19) based on deep features. *Preprints*, 2020030300:2020, 2020.
- Jianpeng Zhang, Yutong Xie, Yi Li, Chunhua Shen, and Yong Xia. Covid-19 screening on chest x-ray images using deep learning based anomaly detection. *arXiv preprint arXiv:2003.12338*, 2020.
- Isabella Castiglioni, Davide Ippolito, Matteo Interlenghi, Caterina Beatrice Monti, Christian Salvatore, Simone Schiaffino, Annalisa Polidori, Davide Gandola, Cristina Messa, and Francesco Sardanelli. Artificial intelligence applied on chest x-ray can aid in the diagnosis of covid-19 infection: a first experience from lombardy, italy. *medRxiv*, 2020.
- Linda Wang and Alexander Wong. Covid-net: A tailored deep convolutional neural network design for detection of covid-19 cases from chest radiography images. *arXiv preprint arXiv:2003.09871*, 2020.
- Xiaosong Wang, Yifan Peng, Le Lu, Zhiyong Lu, Mohammadhadi Bagheri, and Ronald M Summers. Chestx-ray8: Hospital-scale chest x-ray database and benchmarks on weakly-supervised classification and localization of common thorax diseases. In *Proceedings of the IEEE conference on computer vision and pattern recognition*, pages 2097–2106, 2017a.
- RODuda and et al. *Pattern Classification*. 1973.
- P. Lambin and et al. Radiomics: the bridge between medical imaging and personalized medicine. *Nature Reviews*, 12: 749–53, 2017.
- J.J.M. van Griethuysen and et al. Computational radiomics system to decode the radiographic phenotype. *Cancer Research*, 77(21):e104–e107, 2017.
- T. Ojala and et al. A comparative study of texture measures with classification based on feature distributions. *Pattern Recognition*, 29:51–59, 1996.
- J. Schmidhuber. Deep learning in neural networks: An overview. *Neural Networks*, 61:85–117, 2015.
- Katerine Díaz-Chito, Jesús Martínez del Rincón, Marçal Rusiñol, and Aura Hernández-Sabaté. Feature extraction by using dual-generalized discriminative common vectors. *Journal of Mathematical Imaging and Vision*, 61(3):331–351, 2019.
- K Fukunaga. *Introduction to Statistical Pattern Recognition*. Academic Press, Cambridge, 1990.
- J. P. Cohen, M. Luck, and S. Honari. Distribution matching losses can hallucinate features in medical image translation. *preprint arXiv:1805.08841*, 2018.
- A. Krizhevsky, I. Sutskever, and G.E. Hinton. Imagenet classification with deep convolutional neural networks. In *Advances in neural information processing systems*, pages 1097–1105, 2012.
- Y. Li, F.X. Wu, and A. Ngom. A review on machine learning principles for multi-view biological data integration. *Briefings in Bioinformatics*, 19(2):325–340, 2016.
- Vladimir Vapnik. *The nature of statistical learning theory*. Springer science & business media, 2013.
- Joseph Paul Cohen and Henry Z. Lo. Academic torrents: A community-maintained distributed repository. In *Annual Conference of the Extreme Science and Engineering Discovery Environment*, 2014. doi: 10.1145/2616498.2616528. URL <http://doi.acm.org/10.1145/2616498.2616528>.
- Henry Z. Lo and Joseph Paul Cohen. Academic torrents: Scalable data distribution. In *Neural Information Processing Systems Challenges in Machine Learning (CiML) workshop*, 2016. URL <http://arxiv.org/abs/1603.04395>.

Xiaosong Wang, Yifan Peng, Le Lu, Zhiyong Lu, Mohammadhadi Bagheri, and Ronald Summers. Chestx-ray8: Hospital-scale chest x-ray database and benchmarks on weakly-supervised classification and localization of common thorax diseases. In *CVPR*, 2017b.

H. Cevikalp, M. Neamtu, M. Wilkes, and A. Barkana. Discriminative common vectors for face recognition. *IEEE Trans. Pattern Anal. Mach. Intell.*, 27(1):4–13, 2015.